Metamaterial-filled Quarter Circular Microstrip Antenna in the Subwavelength Scale for 3.5 GHz Band Communications

Hao Lu, Xiaofei Xu*, and Hu Wei

School of Communication and Information Engineering
Shanghai University, Shanghai, 200444, China
*xfxu@shu.edu.cn

***Abstract* –** A metamaterial-filled quarter circular microstrip antenna (meta-QCMSA) is proposed for 5G communications in the 3.5 GHz band. Compared with traditional CMSAs, the new meta-QCMSA is superior in its small patch in the subwavelength scale realized by collaboratively using metamaterial and field symmetry techniques. This combination method is observed to be more powerful than a single method solely used. One practical meta-QCMSA is designed and experimentally demonstrated near 3.5 GHz. Its patch length is $0.1\lambda_0$, much smaller than the traditional CMSA. In addition, the compact meta-QCMSA is observed to have a considerable bandwidth of 3.8% and antenna gain of 3.9 dBi in experiments.

***Index Terms* –** Metamaterials, quarter circular microstrip antenna, subwavelength.

I. INTRODUCTION

With the continuous development of 5G/B5G wireless communications [1], compact microwave microstrip antennas (MSAs) [2–3] are of much interest in both academic and industry areas. To make the MSAs smaller, the filling materials for the substrate can have a high relative permittivity (ε_r) and/or permeability (μ_r) by using ceramics and magnets [4–6]. However, these high-index materials are usually difficult to fabricate with low-cost printed circuit board (PCB) technology.

To address the problem, alternative microwave artificial metamaterials [7–17] were proposed in recent decades. These microwave metamaterials do not need high-index ceramics or magnets as substrates. In contrast, they can be realized by using common low-index dielectrics, which are well-compatible with the PCB process. By further loading new functional structures into the low-index dielectrics, the metamaterials may have effective high relative permittivity (ε_{reff}) and/or permeability (μ_{reff}), which are equivalent to the natural high-index materials.

In addition to material technology, there is another useful technique to condense a MSA that takes advantage of electromagnetic (EM) field symmetry for a regular (such as square or circular) patch [2–3]. For instance, regarding the circular MSA (CMSA) operating at its fundamental TM_{11} mode [2], the EM fields in the CMSA cavity are symmetric in different quarters [2]. Hence, according to the uniqueness theorem [18], it is possible to realize a half CMSA (HCMSA) or even a quarter CMSA (QCMSA) (see Fig. 6.7 in [3]) by cutting the original full circle in the CMSA into a half or quarter [2–3] if the boundary conditions are well kept as a magnetic wall or electric wall. Note that the resonant frequencies (f_0s) for these three antennas (CMSA, HCMSA and QCMSA) are almost the same [2–3] if the margin effects are not accounted for. The patch area for the new HCMSA (or QCMSA) is nevertheless only half (or quarter) of the original CMSA.

Metamaterial and EM field symmetry are two independent techniques to shrink traditional MSAs. Inspired by these two techniques, a new compact metamaterial-filled QCMSA (meta-QCMSA) is proposed in this work by synthetically using both technologies. Regarding metamaterial technology, some sector mushroom structures [15] are chosen to fill into the substrate which can be physically constituted from a two-layer substrate. Furthermore, as to form a QCMSA [2–3], the magnetic wall boundary condition is fulfilled by simply using an open edge. The electric wall boundary condition is realized by employing numerous shorting (conducting) pins [2–3].

This combination method is more powerful than a single method solely used. One practical meta-QCMSA was designed for 5G mobile communications in the 3.5 GHz band. It is experimentally demonstrated to resonate at 3.51 GHz (free space wavelength λ_0=85.5 mm, guided wavelength λ_g=57.6 mm). Considering that the dielectric constant for the substrate is 2.2, and the physical length for the quarter circular patch is 8.8 mm, the electrical length is therefore only about $0.1\lambda_0$ or $0.15\lambda_g$ in the subwavelength scale. It is much smaller than the traditional CMSA [2–3] or meta-CMSA [15].

Although with a small patch, the new meta-QCMSA has a considerable bandwidth (BW) of 3.8% and

Submitted On: November 28, 2023
Accepted On: June 10, 2024

https://doi.org/10.13052/2024.ACES.J.390406

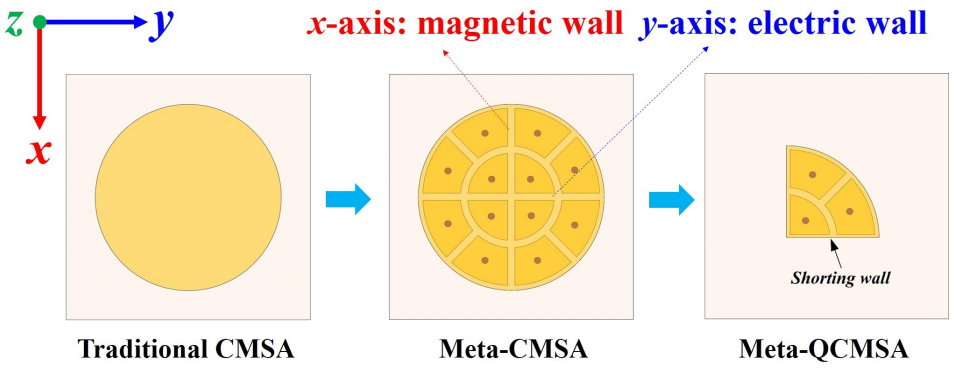

Fig. 1. The designing roadmap of the meta-QCMSA (feedings are not considered).

reasonably high gain of 3.9 dBi in the experimental demonstration. These performances make the new antenna suitable to be applied in 5G/B5G mobile applications.

II. CONCEPT

The subwavelength meta-QCMSA is designed using both the metamaterial substrate and field symmetry techniques. We start from the traditional CMSA [2–3]. A two-step designing roadmap is shown in Fig. 1. First, the traditional CMSA is designed to become a metamaterial CMSA (meta-CMSA) by choosing some particular sector mushroom metamaterial structures [15] to fill into the host low-index dielectric. These mushroom structures were found to be able to increase the ε_{reff} of the antenna. Details for this meta-CMSA can be found in our previous work [15].

Second, on the basis of the meta-CMSA [15], the full circular patch is further reduced to a quarter circle, forming a new meta-QCMSA as proposed in this work. Inspired by the design in [3] (see Fig. 6.7 in [3]), if a CMSA operates at its fundamental TM_{11} mode and the feeding position is along the x-axis, the x-axis can be regarded as the magnetic wall and the y-axis regarded as the electric wall. In a practical antenna, this magnetic wall boundary condition can be fulfilled by directly using an open edge, providing that the antenna is very thin. The electric wall is realized by using numerous shorting (conducting) pins [2–3]. We remark that at the second step, the f_0 for the meta-QCMSA is nearly the same as the meta-CMSA if the margin effects are not accounted for, but its patch area is much reduced. In the following section, we will show the detailed design and results of the conceptual meta-QCMSA.

III. DESIGN AND RESULTS

The configuration of a practical meta-QCMSA is given in Fig. 2. Its overview is shown in Fig. 2 (a), top view in Fig. 2 (b) and side view in Fig. 2 (c). The antenna architecture is similar to [15] but different in the

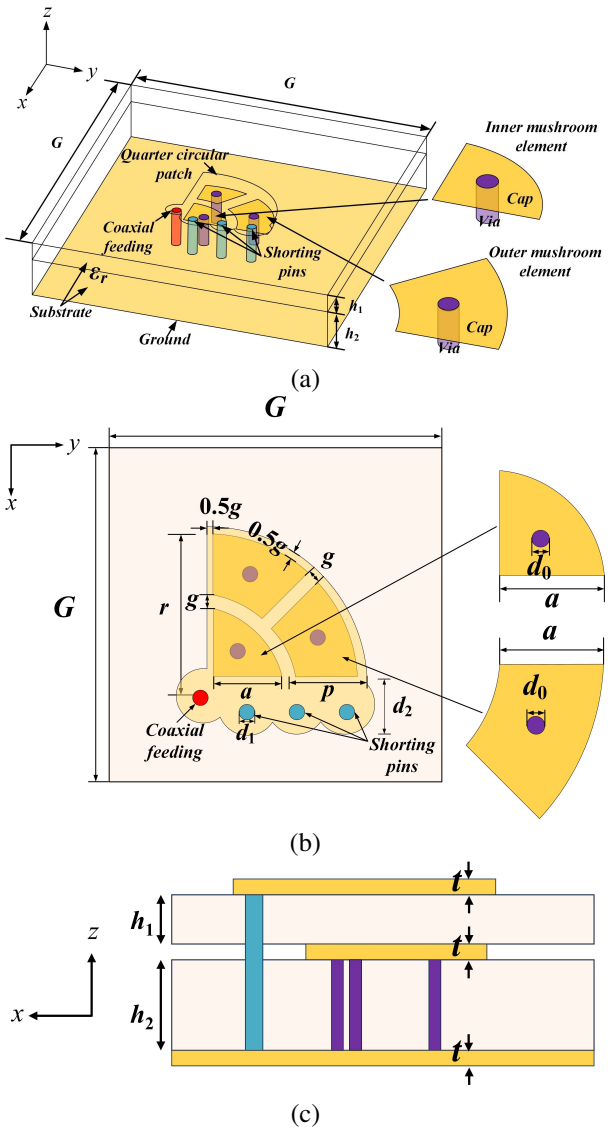

Fig. 2. Configuration of the meta-QCMSA in (a) overview, (b) top view, and (c) side view (feeding is not shown).

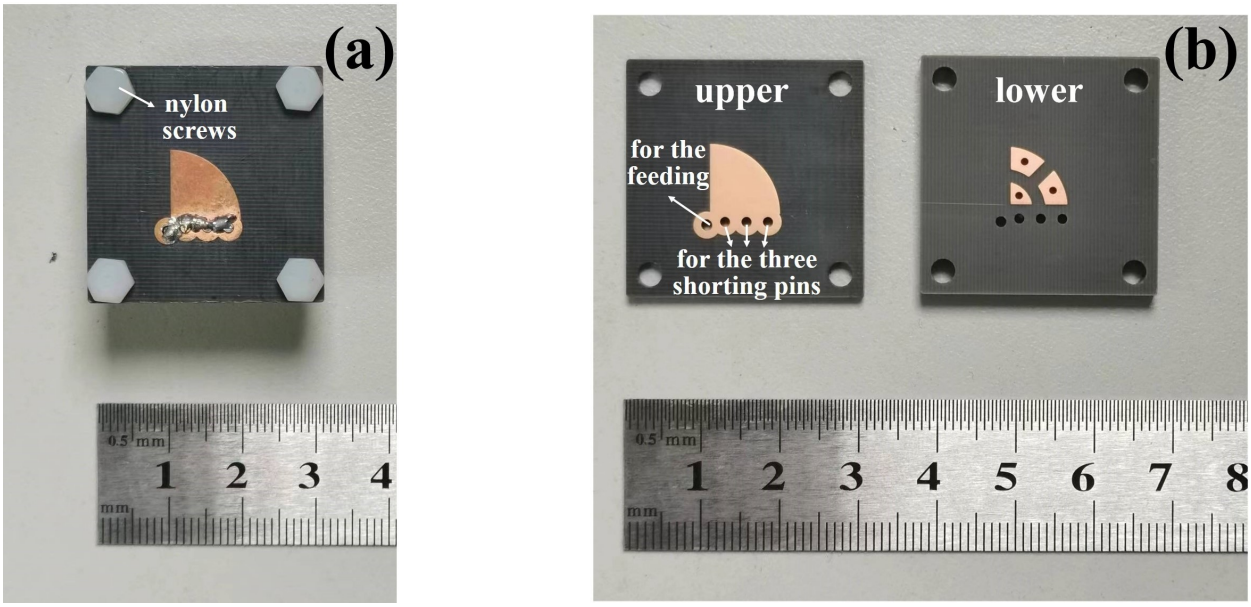

Fig. 3. (a) Antenna sample and (b) upper and lower dielectric layers.

patch shape. Note that the patch is a quarter circular disc herein, and a full disc in [15].

From Fig. 2 (b), we see that the patch radius for the quarter circle (note that it is also the patch length) is r. The ground plane is a square with length G. Beneath the quarter circular patch, there are three sector metallic mushroom elements included in the host substrate. Each mushroom element has a sector-shaped metal cap (with radial length of a) that is linked to the ground plane by a metallic via. The gap between the mushrooms is g. As shown in Fig. 2 (b), the period for the mushrooms along the ρ-axis is p=a+g=r/2.

The host substrate has relative permittivity ε_r and loss tangent tanδ, which is separated by the mushroom caps into two sub-layers with thickness of h_1 and h_2, respectively. The via is supposed with a diameter of d_0 and height of h_2. All three (patch, cap, ground) metal layers have a thickness of t=0.035 mm. Figure 2 (c) clearly shows its vertical profile including the two substrate layers and three metal layers (feeding is not shown).

As illustrated in Fig. 1, the y-axis radius on the edge of the meta-QCMSA is an electric wall. In practical implementations, this electric wall is realized by aligning three shorting pins along the edge. These shorting pins have a diameter of d_1. In addition, to make it easier to solder, each shorting pin is set to be located in a larger soldering pad with a diameter of d_2 (d_2>d_1). The antenna is fed by a 50 Ω coaxial SMA probe at the left lower corner of the quarter circular patch.

We now consider a meta-QCMSA with the following default parameters: r=8.8 mm, G=30 mm, ε_r=2.2, tanδ=0.001, h_1=2 mm, h_2=4 mm, d_0=1 mm, d_1=1.2 mm, d_2=3.4 mm, p=4.4 mm, a=2.8 mm and g=1.6 mm. The metals are all copper with a conductivity of 5.8×10^7 S/m.

The meta-QCMSA is experimentally demonstrated with the above parameters. The antenna sample is shown in Fig. 3 (a), which is assembled from two dielectric layers as shown in Fig. 3 (b). Generally, it needs four steps to realize such a practical antenna. First, the two dielectric layers are fabricated using the PCB process that work as the upper and lower layer, respectively, for the antenna. The dielectric layers are both with nominal ε_r=2.2 and tanδ=0.001, provided by Taizhou Wangling Corp. Second, the two dielectric layers in Fig. 3 (b) are manually assembled using nylon screws located at the four corners of the boards. The third step is to add three solid shorting pins along the patch edge, which are subsequently soldered to connect the quarter patch and ground plane. The fourth (final) step is to solder the coaxial SMA probe that feeds the antenna.

The simulated and measured S_{11} results for the meta-QCMSA are given in Fig. 4 (a). It is observed that the simulated f_0 for the meta-QCMSA is 3.5 GHz from the numerical solver HFSS. The measured f_0 is however slightly upshifted to 3.51 GHz. By normalizing r (8.8 mm) to the λ_0 (85.5 mm) or λ_g (57.6 mm) at 3.51 GHz, we conclude that the patch radius is nearly $0.1\lambda_0$ or $0.15\lambda_g$ for this meta-QCMSA. The simulated BW is 168 MHz (4.8%) while the measured one is 135 MHz (3.8%) from 3.445 to 3.58 GHz. The reduction in BW is attributed to the imperfection of the antenna sample, which results in an increased S_{11} level in the experiment.

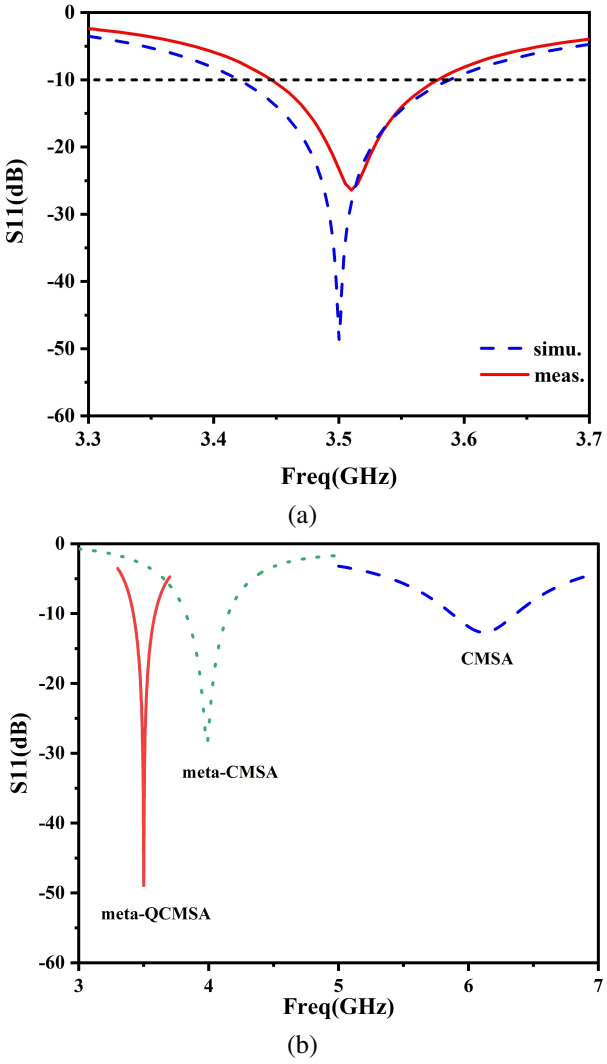

Fig. 4. (a) S_{11} for meta-QCMSA, and (b) a comparison of CMSA, meta-CMSA and meta-QCMSA.

To better feature the new meta-QCMSA, we also consider the original CMSA [2–3] and meta-CMSA [15]. Note that the patches for the CMSA and meta-CMSA are both full circles with diameter d=2r=17.6 mm. The other parameters are all the same as the meta-QCMSA. The CMSA and meta-CMSA are numerically calculated. Their S_{11} curves, in association with the meta-QCMSA, are shown in Fig. 4 (b). We see that the original simplest CMSA resonates at 6.12 GHz (λ_0=49.0 mm, λ_g=33.1 mm). The patch length is its diameter and is 17.6 mm ($0.36\lambda_0$ or $0.53\lambda_g$). The meta-CMSA however resonates at a lower 3.986 GHz (λ_0=75.3 mm, λ_g=50.7 mm). Its patch length is still the diameter (17.6 mm) normalized as $0.23\lambda_0$ or $0.35\lambda_g$.

We remark that for the new meta-QCMSA, its patch length is the radius of nearly $0.1\lambda_0$. It is much smaller than the CMSA ($0.36\lambda_0$) and meta-CMSA ($0.23\lambda_0$). In addition, we note that the f_0 values for the meta-CMSA and meta-QCMSA in Fig. 5 (b) are close but not exactly equal. This is due to the different margin effects for these two antennas, as one patch is a full circle while the other is a quarter.

As reported in [15], the resonances for the meta-CMSA are greatly affected by the thicknesses h_1 and h_2 (see Fig. 3 in [15]). Herein we observe their effects on the meta-QCMSA. It is numerically studied for different h_1 and h_2 values. Their S_{11} curves are shown in Figs. 5 (a) and (b), respectively. The default thicknesses are h_1=2 mm and h_2=4 mm. As revealed from Fig. 5 (a), f_0 becomes higher when h_1 increases; from Fig. 5 (b), f_0 will be lower when h_2 increases. These trends are consistent with [15].

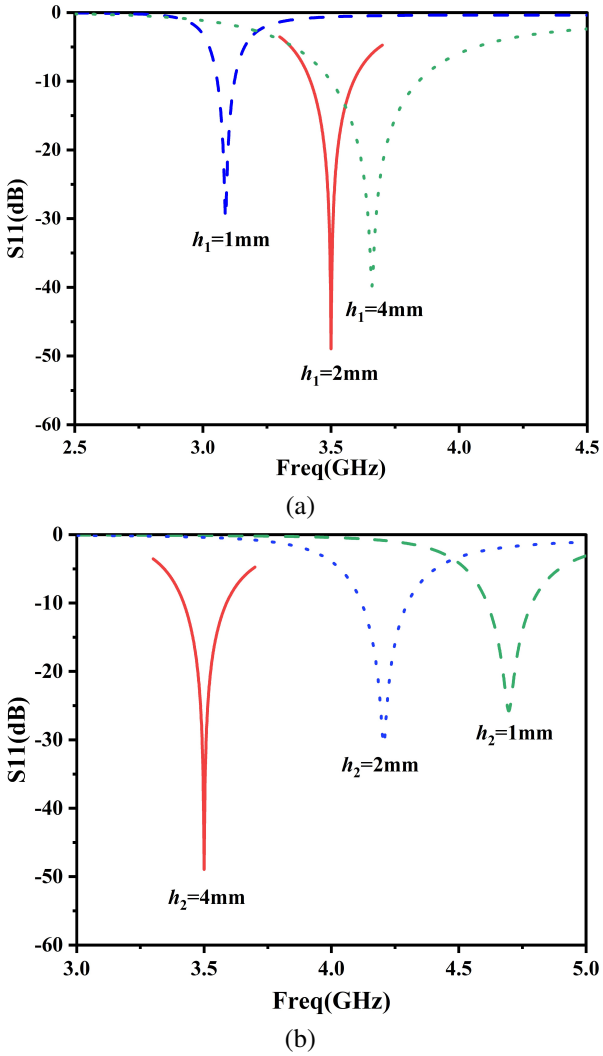

Fig. 5. S_{11} for meta-QCMSA with different (a) h_1 and (b) h_2 values.

The far-field characteristics for the new meta-QCMSA are also evaluated in both simulations and experiments in the microwave chamber. The realized antenna gains are shown in Fig. 6. The peak antenna gain predicted from the numerical solver HFSS is 4.15 dBi. The measured gain values are however slightly lower than simulation in that its peak value is 3.9 dBi. Nonetheless, within the -10 dB impedance BW, the measured antenna gains are all above 2.78 dBi.

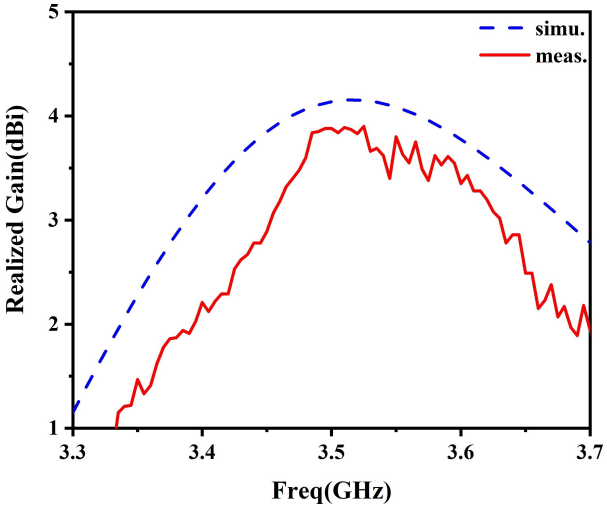

Fig. 6. The realized antenna gains of meta-QCMSA.

Efficiency was not measured. The simulated peak realized efficiency is greater than 90% in HFSS. The radiation efficiency (without considering the mismatching loss) is even higher at over 95% predicted from HFSS.

The radiation patterns of the meta-QCMSA are shown in Fig. 7, obtained at 3.51 GHz. Generally, the simulated and measured co-polarizations are always in good agreement. However, the measured cross-polarizations seem larger than simulation. In addition, it is found that the cross-polarization levels on the H plane (*yoz*) are larger than those on the E plane (*xoz*). In particular, at the bore sight (0°) direction, the measured cross-polarizations on both planes are suppressed lower than -10 dB.

This meta-QCMSA is compared with several other miniaturized MSAs in Table 1. We find that this antenna is featured with a very small patch size ($0.1\lambda_0\times0.1\lambda_0$) while maintaining considerable BW (3.8%) and reasonably high antenna gain (3.9 dBi). As for the antenna in [6], it is smaller ($0.04\lambda_0\times0.05\lambda_0$) than our work by loading a ferrite. However, its antenna gain is very low (-9.06 dBi). In addition, regarding the antennas in the other literatures [8, 10, 12–17], their patch sizes are all larger than this work. The antenna gains are observed to vary

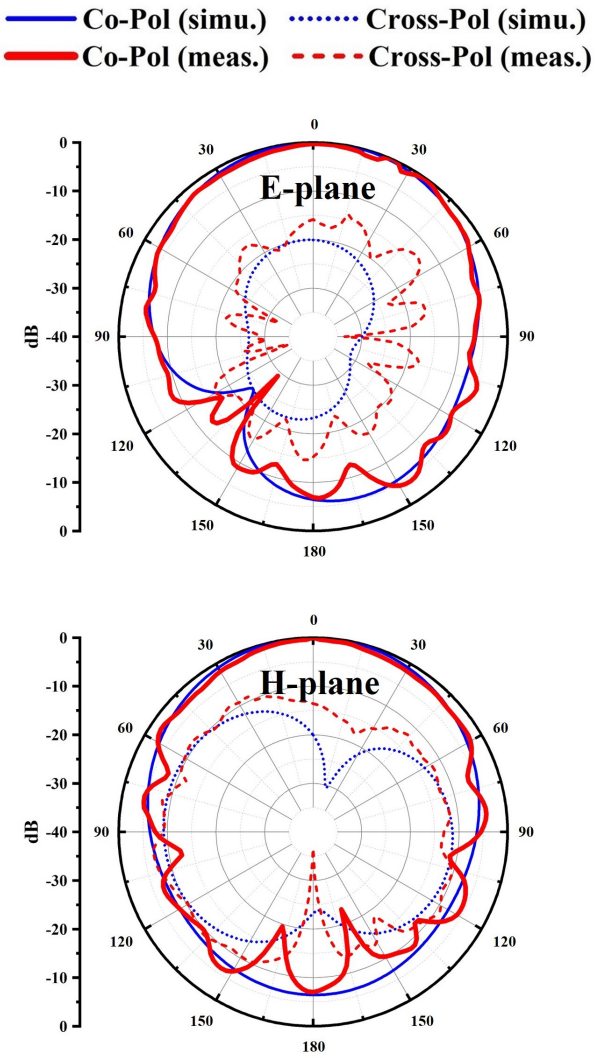

Fig. 7. Radiation patterns at 3.51 GHz.

Table 1: Comparison of several miniaturized metamaterial MSAs

Ref	Patch Size	Thickness	BW	Gain (dBi)
[6]	$0.04\lambda_0\times0.05\lambda_0$	$0.034\lambda_0$	4%	-9.06
[8]	$0.145\lambda_0\times0.203\lambda_0$	$0.008\lambda_0$	0.5%	3.2
[10]	$0.233\lambda_0\times0.233\lambda_0$	$0.018\lambda_0$	3.29%	5
[12]	$0.127\lambda_0\times0.123\lambda_0$	$0.03\lambda_0$	0.93%	2
[13]	$0.20\lambda_0\times0.20\lambda_0$	$0.01\lambda_0$	3.9%	3.71
[14]	$0.23\lambda_0\times0.23\lambda_0$	$0.044\lambda_0$	16.1%	5
[15]	$0.232\lambda_0\times0.232\lambda_0$	$0.035\lambda_0$	3%	5.9
[16]	$0.19\lambda_0\times0.19\lambda_0$	$0.11\lambda_0$	-	4.76
[17]	$0.17\lambda_0\times0.25\lambda_0$	0.026λ	7.22%	1.94
This work	$0.1\lambda_0\times0.1\lambda_0$	$0.07\lambda_0$	3.8%	3.9

from 2 to 5.9 dBi, which are in the same order of this meta-QCMSA.

IV. CONCLUSION

A subwavelength meta-QCMSA is designed by jointly using metamaterial and field symmetry techniques. One practical meta-QCMSA is demonstrated in both full-wave simulations and experiments, operating at the 3.5 GHz band. The patch length for the meta-QCMSA is about $0.1\lambda_0$ or $0.15\lambda_g$. The BW, antenna gain and radiation patterns for the new antenna are also studied in the experiments, which can promisingly meet the demands of portable devices for 3.5 GHz communications.

ACKNOWLEDGMENT

This work was supported by the National Natural Science Foundation of China (No. 11904222).

REFERENCES

[1] 3GPP TS 38.104, V17.5.0 [Online]. Available: https://www.3gpp.org.

[2] R. Garg, P. Bhartia, I. Bahl, and A. Ittipiboon, *Microstrip Antenna Design Handbook*. Boston: Artech House, 2001.

[3] G. Kumar and K. P. Ray, *Broadband Microstrip Antennas*. Boston: Artech House, 2003.

[4] J. S. Kula, D. Psychoudakis, W.-J. Liao, C.-C. Chen, J. L. Volakis, and J. W. Halloran, "Patch-antenna miniaturization using recently available ceramic substrates," *IEEE Antennas and Propagation Magazine*, vol. 48, pp. 13-20, 2006.

[5] W. Lee, Y. Hong, H. Won, M. Choi, K. Isbell, J. Lee, T. Kim, and S. Park, "Lossy ferrite core-dielectric shell structure for miniature GHz axial-mode helical antenna," *IEEE Antennas and Wireless Propagation Letters*, vol. 18, pp. 951-955, 2019.

[6] S. Jemmeli, T. Monediere, E. Arnaud, and L. Huitema, "Ultra-miniature and circularly polarized ferrite patch antenna," *IEEE Transactions on Antennas and Propagation*, vol. 71, pp. 6435-6443, 2023.

[7] S. Jahani, J. Rashed-Mohassel, and M. Shahabadi, "Miniaturization of circular patch antennas using MNG metamaterials," *IEEE Antennas and Wireless Propagation Letters*, vol. 9, pp. 1194-1196, 2010.

[8] F. Farzami, K. Forooraghi, and M. Norooziarab, "Miniaturization of a microstrip antenna using a compact and thin magneto-dielectric substrate," *IEEE Antennas and Wireless Propagation Letters*, vol. 10, pp. 1540-1542, 2011.

[9] B. Zarghooni, A. Dadgarpour, and T. A. Denidni, "Greek-key pattern as a miniaturized multiband metamaterial unit-cell," *IEEE Antennas and Wireless Propagation Letters*, vol. 14, pp. 1254-1257, 2015.

[10] T. Cai, G. Wang, X. Zhang, Y. Wang, B. Zong, and H. Xu, "Compact microstrip antenna with enhanced bandwidth by loading magneto-electro-dielectric planar waveguided metamaterials," *IEEE Transactions on Antennas and Propagation*, vol. 63, pp. 2306-2311, 2015.

[11] M. Li, K. Luk, L. Ge, and K. Zhang, "Miniaturization of magnetoelectric dipole antenna by using metamaterial loading," *IEEE Transactions on Antennas and Propagation*, vol. 64, pp. 4914-4918, 2016.

[12] Q. Huang, X. Xu, and R. Zhang, "Study of the combination method and its application to shrink a patch antenna operating in the UHF band," *Applied Computational Electromagnetics Society Journal*, vol. 37, pp. 209-214, 2022.

[13] S. Painam and C. Bhuma, "Miniaturizing a microstrip antenna using metamaterials and metasurfaces," *IEEE Antennas and Propagation Magazine*, vol. 61, pp. 91-135, 2019.

[14] S. Liu, Z. Wang, and Y. Dong, "Compact wideband SRR-inspired antennas for 5G microcell applications," *IEEE Transactions on Antennas and Propagation*, vol. 69, pp. 5998-6003, 2021.

[15] H. Lu, G. Dai, X. Xu, and X. Deng, "Miniaturized circular microstrip antenna designed with quasi-periodic sector metamaterials," *Microwave and Optical Technology Letters*, vol. 64, pp. 1614-1620, 2022.

[16] H. Lu and X. Xu, "Comparative study of miniaturized microstrip antennas designed with different super-substrate materials operating at 900 MHz," *Applied Physics A*, vol. 128, p. 297, 2022.

[17] M. Ameen and R. K. Chaudhary, "ENG-TL inspired dual-polarized antenna using curved meander, two-arm Archimedean spirals and CSRR mushroom," *Microwave and Optical Technology Letters*, vol. 65, pp. 1778-1786, 2023.

[18] C. A. Balanis, *Advanced Engineering Electromagnetics*. Hoboken: Wiley, 2012.

Hao Lu was born in Hubei, China, in 1998. He received the M.S. degree from Shanghai University, Shanghai, China, in 2023. His research interest includes antenna miniaturization technology.

Xiaofei Xu received the B.S. degree in 2007 and the Ph.D. degree in 2011, both from Nanjing University, Nanjing, China. He is currently with the School of Communication and Information Engineering in Shanghai University, Shanghai, China.

Dr. Xu's research areas include electromagnetics, antennas and microwave technology. He has authored over 50 papers published in peer-reviewed journals and conference proceedings. He also serves a number of journals and society workshops as the reviewer or organizer.

Hu Wei was born in Anhui, China, in 1998. He is currently pursuing the M.S. degree from Shanghai University, Shanghai, China. His research interest includes antenna technology.